Preliminary CFD Study on Free Jet Flow at the Marviken Test Facility

Gong Hee Lee*, Seon Ho Choi Reactor System Department, Korea Institute of Nuclear Safety, Daejeon, 34142, Korea

*Corresponding author: ghlee@kins.re.kr

*Keywords: computational fluid dynamics, free jet, high-energy pipe rupture, jet impingement, validation

1. Introduction

When a high-energy pipe rupture occurs in a nuclear power plant, the resulting jet impingement can cause failure and severe damage to adjacent safety-related structures, systems, and components (SSCs) [1]. To design effective protection systems for mitigating such damage, the dominant flow phenomena must be sufficiently understood and accurately modeled [1].

According to Appendix A of the Standard Review Plan (SRP) 3.6.2 [2], potential non-conservatisms were identified in the jet modeling approach described in the ANSI/ANS 58.2 Standard [3], particularly regarding (a) the strength of the jet, (b) the extent of the zone of influence, and (c) the spatial and temporal variation of loading effects resulting from postulated high-energy pipe ruptures on neighboring structures, systems, and components (SSCs).

In this study, a preliminary computational fluid dynamics (CFD) analysis of free jet flow at the Marviken test facility was performed to assess the applicability of the ANSYS CFX software. Furthermore, the characteristics of the free jet flow were examined with respect to variations in nozzle inlet pressure and temperature.

2. Analysis Model

The Marviken Jet Impingement Test Program [4] was initiated to acquire experimental data on the spatial distribution of pressure and temperature in the free jet flow, as well as the force distribution exerted on target SSCs.

Fig. 1 shows a schematic diagram of the analysis model (test number 05; free jet case) used in this study. The model consists of a nozzle, a central probe and a downstream pipe spool. Assuming symmetric jet flow behavior, a symmetry boundary condition was applied to reduce computational time. The computational domain extends 20.68 m in the axial direction and 7 m in the radial direction. The nozzle has a diameter (D) of 0.299 m and a length (L) of 1.18 m. A central probe with a diameter of 0.1 m is installed along the jet centerline to measure pressure and temperature. For simplicity, both the horizontal structural support beams and the horizontal instrumentation beams were excluded from the analysis model.

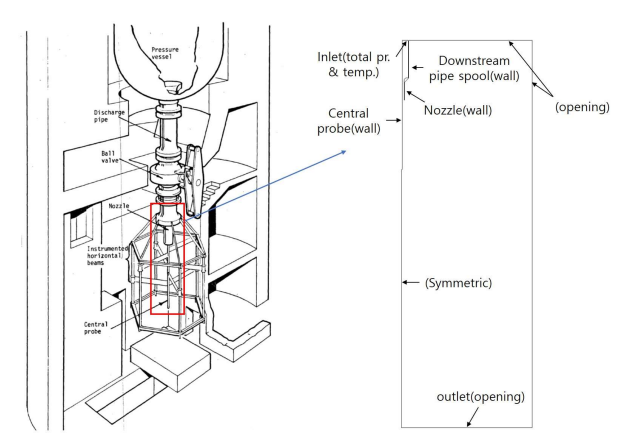


Fig. 1. Analysis model : computational domain & boundary conditions [4].

During the time period from 0 s to 82 s, only steam flow was present. Therefore, the Peng–Robinson real gas model was selected to predict the thermodynamic properties of the steam flow.

3. Numerical Modeling

The free jet flow was assumed to be steady, compressible, turbulent, and single-phase. For reference, the numerical methods and boundary conditions adopted in this study are summarized in Table I.

Table I: Numerical methods and boundary conditions for flow analysis

Numerical methods		Note
Discretization accuracy for convection term	Momentum eqn.	High resolution
	Turbulence eqn.	High resolution
Turbulence model		SST k-ω
Velocity-pressure coupling		Rhie Chow (4 th order)
Real gas model		Peng-Robinson
Near wall treatment		Automatic wall treatment
Convergence criteria		< 10 ⁻⁵
Boundary conditions		Note
1	Total pressure	(see Fig. 2)
Inlet T	tal temperature	(see Fig. 2)
	Turbulence	medium intensity (5%)
Outlet		Opening
Top plane, Side plane		Opening
Center plane		Symmetric
Wall		No-slip & smooth wall

Hexahedral elements were generated using ICEM-CFD. A total of approximately 9.2 × 10⁵ elements was employed in the simulations. To accurately capture the free jet flow and associated shock structures—such as Mach disks, shock reflection zones, and shear layers—a refined mesh was applied near the above-mentioned critical regions, including the nozzle exit and adjacent wall surfaces. This meshing strategy is generally recommended for high-speed jet flow simulations.

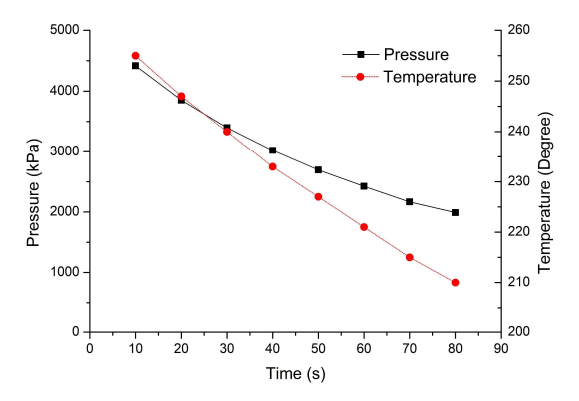


Fig. 2. Pressure and temperature magnitudes at the nozzle inlet.

4. Results and Discussion

The pressure distribution within the jet flow characterizes the jet strength [1]. The impingement force can be determined by integrating the local stagnation pressure over the surface of the target SSCs [1]. Accordingly, pressure distribution is one of the key parameters in evaluating jet impingement effect.

Fig. 3 presents the static pressure distribution along the axial direction from the nozzle exit. A rapid decrease in static pressure is observed within one nozzle diameter downstream of the nozzle exit.

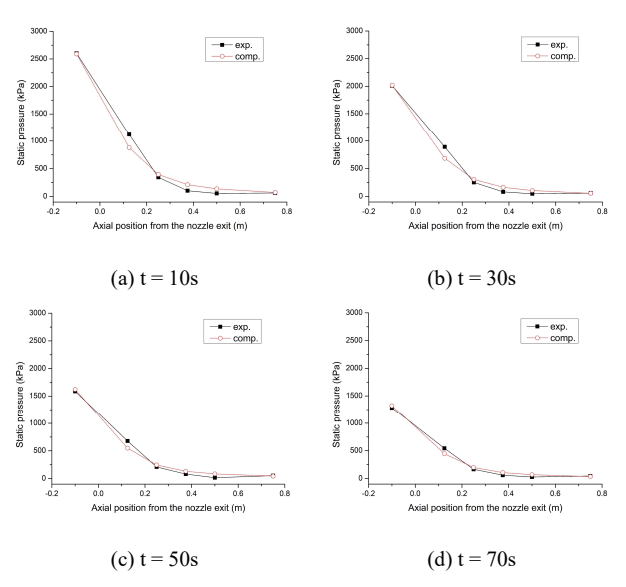


Fig. 3. The static pressure distribution along the axial direction from the nozzle exit.

The calculated static pressure profile showed good qualitative agreement with the experimental data.

Fig. 4 shows the calculated Mach number distribution for various nozzle inlet pressure conditions. As the inlet pressure increases, the pressure ratio between the nozzle and the ambient environment also increases, resulting in stronger expansion through the nozzle. This leads to a larger jet spread angle and higher Mach numbers downstream of the nozzle exit. The presence of Mach disks, as well as significant velocity deceleration in the region behind the Mach disk, was clearly captured in the simulation results.

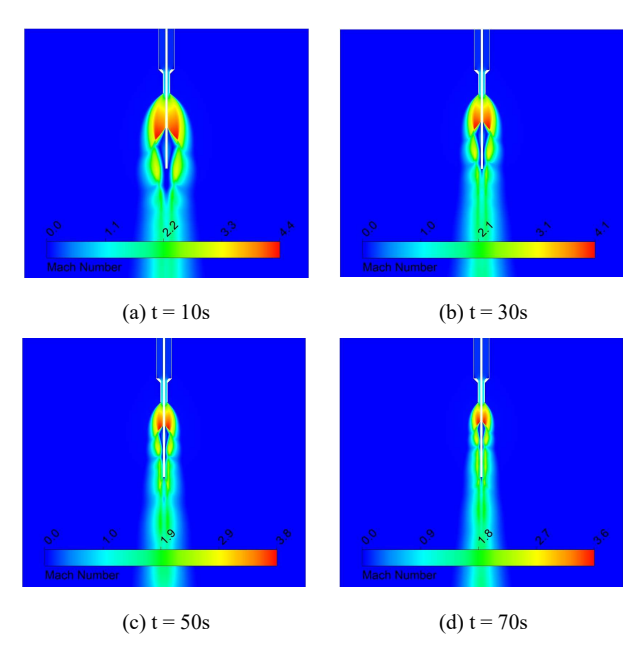


Fig. 4. The calculated Mach number distribution for various nozzle inlet pressure conditions.

Fig. 5 illustrates the calculated distribution of turbulence kinetic energy (TKE) for various nozzle inlet pressure conditions. Regions of high turbulence kinetic energy (TKE) are typically observed at shock—shear layer interaction zones and within the mixing layers. When shock cells interact with turbulent shear layers, turbulence is amplified due to compressibility effects and shock-induced instabilities. As the jet flow develops, entrainment of ambient air enhances mixing, particularly in the outer shear layers. The mixing layer continues to generate and sustain turbulence further downstream, although its intensity gradually diminishes with distance.

In contrast, regions of low TKE are generally located within the jet core, especially near the centerline and immediately downstream of the nozzle exit. In this region, the velocity remains nearly uniform and exhibits low turbulence levels until the onset of jet breakdown.

5. Conclusions

Based on the preliminary CFD analysis of the free jet flow conducted at the Marviken test facility, the following key conclusions can be drawn:

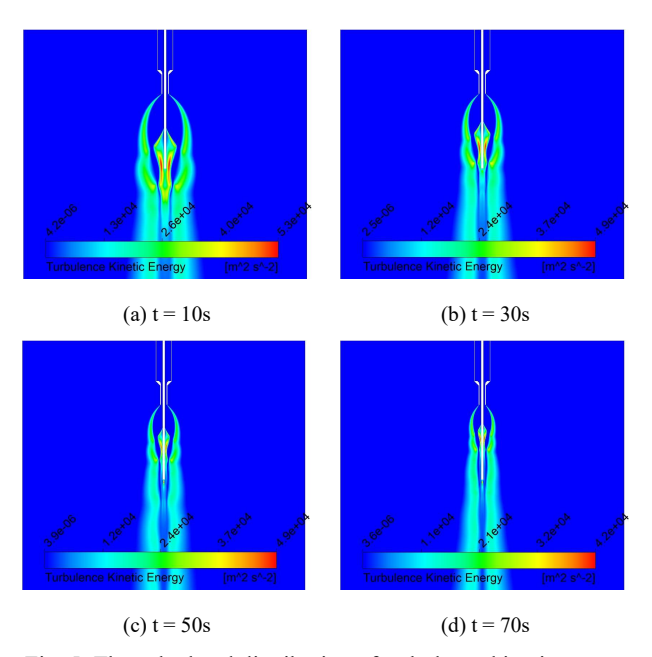


Fig. 5. The calculated distribution of turbulence kinetic energy (TKE) for various nozzle inlet pressure conditions.

- (1) It was found that the calculated static pressure profile along the axial direction from the nozzle exit showed good qualitative agreement with the experimental measurements.
- (2) An increase in nozzle inlet pressure leads to a larger jet spread angle and higher Mach numbers downstream of the nozzle exit.

DISCLAIMER

The opinions expressed in this paper are those of the author and not necessarily those of the Korea Institute of Nuclear Safety (KINS). Any information presented here should not be interpreted as official KINS policy or guidance.

ACKNOWLEGEMENT

This work was supported by the Korea Institute of Nuclear Safety (A3FD25030, A6FD25021 & A3EI25034).

REFERENCES

- [1] S. Kim, M. Ishii, R. Kong, Jet Impingement in High-Energy Piping Systems, 2021, USNRC, NUREG/CR-7275.
- [2] USNRC, Determination of Rupture Locations and Dynamic Effects Associated with the Postulated Rupture of Piping, 2016, Standard Review Plan 3.6.2, NUREG-0800.
- [3] American Nuclear Society, Design Basis for Protection of Light Water Nuclear Power Plant against the Effects of Postulated Pipe Rupture, 1988, ANSI/ANS-58.2.
- [4] Nuclear Energy Agency, The Marviken Full Scale Jet Impingements Tests: Test 5 Results, 1981, MXD-205.